Preparation and Optimization of Mordenite Nanocrystal-Layered Membrane for Dehydration by Pervaporation

Yaqi Zhang, Yuta Nakasaka*, Teruoki Tago, Aya Hirata, Yuki Sato and Takao Masuda

Division of Chemical Process Engineering, Faculty of Engineering, Hokkaido University, N13W8 Kita-ku, Sapporo 060-8628, Japan

* Corresponding author

TEL: (+81)-11-706-6552

FAX: (+81)-11-706-6552

E-mail: nakasaka@eng.hokudai.ac.jp

Keywords: Mordenite nanocrystal-layered membrane, Pervaporation, Water/organic solutions, Pre-aging

ABSTRACT

Mordenite nanocrystal-layered membranes consisting of a mordenite nanocrystal layer and protection layer were successfully prepared. The obtained mordenite membranes were applied to the separation of water from water/organic solutions (organic solvents: ethanol, acetone, iso-propanol, or acetic acid) using a pervaporation method at temperatures from 60 to 100 ºC. Water permeance through the mordenite membrane in each water/organic solution system was almost identical regardless of organic solvent types in the feed solution. In contrast, the permeance of the organic molecules depended on their polarities. The pre-aging temperature of the mother liquid and the heating rate for formation of the protection layer affected the secondary growth process that formed the protection layer, leading to different morphologies and sizes of the crystals in the protection layer. Water flux increased with decreasing crystal size in the protection layer because the number of non-zeolitic pores among the mordenite crystal increased as the crystal size decreased.

1. Introduction

Due to increased demand for chemical products and concerns about depletion of fossil fuel resources, diversification of feedstocks for petrochemical products is of great interest, and production of useful chemicals from biomass is being explored. However, the large amount of water in biomass can make isolation of chemicals difficult. In chemical processes, liquid mixtures are usually separated by distillation, which utilizes the vapor-liquid equilibrium difference. Purification of chemicals derived from biomass, such as ethanol, acetic acid, and acetone [1], requires a distillation column with a large number of plates and a high reflux ratio, plus a complex process for purification of azeotropes, which consumes a large amount of energy. Thus, a new high-purity, low-energy consumption separation process is needed. A pervaporation technique is a promising technique to achieve this goal.

Pervaporation using zeolite membranes has been studied because of the greater chemical and hydrothermal stability of the zeolite membranes compared to polymer membranes [2, 3]. Permeability of water through several types of zeolite membranes, *e.g.*, zeolite A [4-6], ZSM-5 [7-11], mordenite [12-14], and others [15-17], from a water/organic solution has been investigated. Water molecules in the solution adsorb into the membrane, permeate through it, and are removed as vapor. Therefore, the hydrophilic properties of the membrane, *e.g.*, Si/Al ratio of zeolites, are important because water separation depends on selective adsorption to the hydrophilic sites of the membrane [18]. However, for zeolites containing Al_2O_3, dealumination proceeds in acidic solutions, decreasing the separation factor due to generation of defects with long-term use.

In these zeolite membranes, because mordenite possesses resistance to acidic solutions [19], a mordenite membrane is a promising candidate as the separation membrane for acidic solutions [12, 13]. The high concentration of Al within the framework of the mordenite structure allows the mordenite membrane to separate water from water-acetic acid mixtures due to its high hydrophilicity. Moreover, the membrane performance could be improved by controlling the crystal morphology composing the membrane during the secondary growth process [20, 21].

Meanwhile, a pre-aging treatment, which is defined as the mixing of reagents before onset of heating to crystallization temperature, can control the morphology and size of the zeolite crystal [22]. Chen et al. [23] reported morphology control of the zeolite crystal by a pre-aging treatment during preparation of a silicalite membrane.

The main objective of the present study was to prepare a mordenite membrane and investigate its ability to separate water from water/organic solutions by pervaporation. We have previously reported the preparation of a silicalite-1 membrane composed of silicalite-1 protection layer, silicalite-1 nanocrystal layer and porous alumina filter [27, 28], in which the application of nano-sized silicalite-1 crystal as a seed crystal was effective in improving the membrane performance. Compared with the dense membrane prepared by in situ hydrothermal synthesis methods, the water flux of the layer membrane prepared using the nanocrystals with a diameter of 60 nm was approximately 100 times high. In the present study, nano-sized mordenite crystals [29] were used as the seeds. Finally, the effect of a pre-aging treatment on the membrane morphology and membrane performance was examined.

2. Experimental

2.1. Preparation of mordenite nanocrystal-layered membranes

Mordenite nanocrystals (Si/Al=12.5) approximately 120 nm in size were prepared *via* hydrothermal synthesis in a water-surfactant-oil solution. An aqueous solution containing Si and Al was prepared by hydrolysis of tetraethylorthosilicate (Si source, Wako Chemicals) and aluminum isopropoxide (Al source, Wako Chemicals) with a dilute aq. tetraethyl-ammonium-hydroxide (TEA-OH) solution (Wako Chemicals) at room temperature. Polyoxyethylene-(15)-oleyl ether (O-15, Nikko Chemicals) and cyclohexane were employed as a surfactant and organic solvent, respectively. Detailed information on the preparation of mordenite nanocrystals has been reported previously [29].

A cylindrical alumina ceramic filter (NGK insulators, LTD.) was used as a membrane support. The inner and outer diameters and the length of the filter were 6 mm, 11 mm, and 50 mm, respectively. This filter was constructed in two porous regions; the pore diameter of the inner region was about 2-3 μm (rough region), and the outer region was dense and its pore diameter was 0.1μm. The filter was immersed in a 0.1 N hydrochloride solution for 6 h, and washed in distilled water. The mordenite nanocrystals were dispersed ultrasonically in an alkaline (approximately pH 12) aqueous solution at a concentration of 5.8 $g \cdot m^{-3}$. The dispersed nanocrystals were layered on the outer surface of cylindrical alumina ceramic filters using a filtration method under low-pressure vacuum on the permeate side. The thickness of the nanocrystal layer is about 8μm. To

protect the nanocrystal layer against mechanical shock, a protection layer with micrometer-sized mordenite was formed hydrothermally (secondary growth) on the nanocrystal layer without organic structure directing agents (OSDA). An aqueous solution (mother liquid) containing Si and Al sources prepared by of tetraethylorthosilicate and aluminum isopropoxide was used to form the protection layer and the molar composition was: SiO_2:Na_2O:Al_2O_3:H_2O=1:0.32:0.04:111. The aqueous solution was stirred at room temperature, 60 °C and 80 °C for24 h, as pre-aging treatment. Then the alumina filter with a mordenite nanocrystal layer was immersed in the precursor solution and heated to 150-200 °C with heating rate of 4.2-8.3 °C/h and kept at the hydrothermal temperature for 0-12 h to form the protection layer on the nanocrystal layer.

The powders obtained in the solution during hydrothermal synthesis for the protection layer of mordenite membrane were characterized by X-ray diffraction (XRD, JEOL JDX-8030) and X-ray Fluorescence Analysis (XRF, Rigaku Supermini) for the detection of the Si/Al ratio in the mordenite crystals. The membrane morphology and composition (Si/Al ratio) were characterized by scanning electron microscopy (SEM, JEOL JSM-6500F) and energy dispersive X-ray spectroscopy (EDS, JEOL JSM-6510LA), respectively.

2.2. Pervaporation experiments

Pervaporation experiments were conducted using a conventional method at temperatures ranging from 60 to 100 °C using the stainless-steel autoclave vessel shown in Fig. 1. Water/organic solutions (organic solvent: ethanol, iso-propanol, acetone, or

acetic acid) were used as feed solutions for the pervaporation experiment. Concentrations of the water/organic solutions and dielectric constants of organic solvents used are listed in Table 1. The new water/organic solutions were used at each pervaporation temperature. The acid-stability of the membranes was checked by pervaporation experiments using water/acetic acid mixture (acetic acid concentration is 90 wt %) as a feed solution. The water/acetic acid solution was renewed at every 6 h and the whole pervaporation experiments were continuous to carry out for 32.6 h. After the membrane was immersed in the feed solution, nitrogen was fed into the gas phase of the vessel at room temperature to replace the air. The vessel was then heated to pervaporation temperatures. Molecules that permeated through the membrane were swept out with the nitrogen. The composition of the exit gas obtained from the permeate side of the membrane was analyzed using an on-line gas chromatograph equipped with a Porapak-Q column and TCD and FID detectors. The procedure has been described in detail previously [27, 28].

[Figure 1 and Table 1]

The separation factor, α, is defined as:

$$\alpha = \frac{F_w / F_o}{C_w / C_o} \qquad (1)$$

where F_w and F_o are the molar flux of water and organic solvent on the permeate side, respectively, and C_w and C_o are the molar concentrations of water and organic solvent, respectively, on the feed side. The total amount of water and organic solvent permeating through the membrane during each experiment was less than 3%. Accordingly, the initial concentrations of C_w and C_o were used to calculate the separation factor.

The permeance, P_i, is defined as:

$$P_i = \frac{F_i}{C_i} \qquad (2)$$

F_i is the molar flux of water or organic molecules that permeate through the mordenite nanocrystal-layer membrane and C_i stands for the molar concentration of water or organic solvent in the feed side solution. The permeance indicated the permeability of the component (water or organic molecules) in the organic solution through the mordenite nanocrystal-layer membrane.

3. Results and Discussion

3.1 Synthesis of the mordenite nanocrystal-layered membrane

Figure 2 shows FE-SEM photograph of a cross-sectional area of mordenite nanocrystal-layered membrane in which the protection layer was formed at a hydrothermal temperature of 180 °C and hydrothermal period of 12 h. Table 2 shows the pre-aging temperature, pre-aging period, and heating rate from pre-aging temperature to the hydrothermal temperature. A protection layer with micrometer-sized crystals was formed on the nanocrystal layer with a thickness of about 5μm. The crystal size in the protection layer was much larger than that in the nanocrystal layer, indicating that secondary growth of mordenite nanocrystals occurred during formation of the protection layer.

[Figure 2]

The effect of the hydrothermal temperature on mordenite protection layer formation and its separation properties was examined to determine the appropriate hydrothermal temperature. Hydrothermal temperatures of 150, 180, and 200 °C were used for the formation of the protection layer. Figure 3 shows the XRD patterns of the powder samples obtained during protection layer formation and commercial mordenite. Powder samples synthesized at 150 °C and 180 °C showed the same pattern as the commercial mordenite. On the other hand, the powder sample synthesized at 200 °C possessed low crystalline mordenite containing an impurity phase which was ascribed to moganite type crystal, indicating that there was a possibility to form other crystal types in the protection layer during the synthesis. In some cases, the structure of the powder is not exactly the same as the crystals constituting the membrane layer [30]. Accordingly, all of these membranes were used for separation of water from a water/iso-propanol solution by pervaporation at 80°C and water fluxes and separation factors are listed in Table 2. From the table, all of the membranes possess the water separation ability and the separation factor are more than 500 in each membrane, and the membrane synthesized at 180 °C exhibited better separation properties and permeability compared with the membrane obtained at 150 °C and 200°C. Therefore, all of the membranes discussed below were prepared at the hydrothermal temperature of 180 °C

As mention above, the mordenite possesses resistance to the acidic solution. The membrane acid stability was examined by separation of water from acetic acid/water solution (acetic acid concentration is 90 wt%) by pervaporation. The membrane was prepared at the hydrothermal temperature of 180 °C. Table 3 shows the water flux and

separation factor of the membrane during the pervaporation experiment at 100 °C. As shown in the table, the membrane maintained the separation performance for 32.6 h even at the high acetic acid concentration. Li et al. [13] did the same pervaporation experiment to test the acid stability of the mordenite membranes. A separation factor of 50 was obtained when the membrane used for separating water from water/acetic acid mixtures (acetic acid concentration is 90 wt%). Compared with the A-type zeolite membranes, although lower in the water fluxes and separation factors, the acid stability makes mordenite membranes good candidates for the separation of acid mixtures and wide usage in organic dehydration.

[Table 2, Table 3]

3.2 Effect of organic polarity in feed on water and organic solvent permeation

Water molecules permeate through the mordenite nanocrystal-layered via membrane water-acid site networks because water molecules have high polarity and selectively adsorb on the acid site of mordenite. Meanwhile, polar organic molecules, which have high affinity with acidic sites, affect the permeance of organic solvents and the separation factor. To investigate the effect of organic solvent polarity on the permeance of water and organics through the membrane, dielectric constants were used to evaluate the polarity of the organic solvents. Dielectric constants of each organic solvent are listed in Table 1. A greater dielectric constant value indicates greater polarity.

Figure 4 shows the relationship between the permeance of each component through the mordenite nanocrystal-layered membrane and the dielectric constant of the organic

solvent. The greater water permeance of nearly 10^3 times than organic molecules in all of the water/organic systems proved that the mordenite nanocrystal-layered membrane possess high water separation ability from the mixtures. Since the high Al element existed in mordenite zeolite structure generated high hydrophilicity, water molecules have higher affinity to the mordenite surface compared with organic molecules. Moreover, water permeance from a water/organic solution through a membrane was identical regardless of the organic solvent in the feed, and exhibited nearly the same value as the permeance of water through a membrane from a pure water solution (*i.e.*, without organic solvent), indicating that the dominant mechanism of the permeation of water is the same regardless of coexisting organic molecules.

Table 1 shows the apparent activation energies of water flux through the membranes from the water/organic solutions. The apparent activation energies of water flux through the membranes from pure water (without an organic solvent) are also showed for comparison. The apparent activation energies of water flux through the mordenite nanocrystal-layered membrane were similar regardless of the organic solvent in the feed and were close to the apparent activation energy of water flux through the membrane from a pure water feed. The apparent activation energy of water flux through the hydrophilic silicalite-1 nanocrystal-layered membrane from water/acetone solution (acetone concentration is 90 wt%) [27, 28] was 35 kJ/mol and the value was similar to that of the mordenite nanocrystal-layered membrane. In the hydrophilic silicalite-1 nanocrystal-layered membrane, water-silanol networks that formed on non-zeolitic pore spaces among the crystals acted as the main channel for water permeation, and the interface between the nanocrystal layer and protection layer was important for the

separation because this area became the densest area in the membrane [28]. Since the mordenite membrane was prepared by the same procedure as the silicalite-1 membrane [28], it was considered that there were some non-zeolitic pores among the crystals. During the pervaporation to separate water from water/organic mixtures, water molecules were adsorbed on the surfaces of zeolitic and non-zeolitic pores. As compared with silanol groups on the surface of silicalite-1 crystal, the affinity of water molecules to the surface of mordenite crystal was much higher due to the strong ionic sites. However, since the mordenite membrane showed almost the same activation energy as the slilicalite-1 membrane, the non-zeolitic pores among the crystals, on which the water adsorption layer was formed, were the important channel for water permeation. The water molecules can diffuse through the non-zeolitic pore surrounded by the water adsorption layer, and consequently the size of non-zeolitic pores mainly affects the separation properties.

[Figure 3, Figure 4 and Table 1]

3.3 Effects of pre-aging and heating rate for synthesis of the protection layer on performance of mordenite nanocrystal-layered membranes

Ideally, the zeolite membranes must be continuous with good cross-linking between crystals and free of pinholes and cracks to get high selectivities. However, most of the synthesis procedures render membranes with some intercrystalline gaps and defects [31,

32]. The amount of these crystals and their sizes play an important role in the overall quality of the membranes [33]. It is suggested that the non-zeolitic pores have size distributions and the pores smaller than the zeolite pores may also affect flux and selectivity [34]. Moreover, some studies showed that the non-zeolitic pores are selective for some mixtures and pervaporation separations even positively affected by non-zeolitic pores [35].

In order to investigate the effect of the non-zeolitic pores on membranes quality, mordenite nanocrystal-layered membranes at conditions of hydrothermal period of 0, 12 and 24 h were prepared. Table 4 shows the results of membrane performance of water flux and separation factor as a function of hydrothermal period. In the case of M1, though prepared without hydrothermal period, the membrane exhibited the separation ability. Moreover, the separation factor of membranes (M1, M2, and M3) increased with increasing the hydrothermal period, implying that non-zeolitic pores were exist among the crystals and that the size of the non-zeolitic pore decreased to the appropriate size for water separation. On the other hand, the long hydrothermal period led to the excessive secondary growth of zeolite, thereby resulting in the decrease in water flux. Such an appropriate pore space was expected to be formed around the interface between the nanocrystal and protection layers [28].

The morphology and crystal size around the interface formed by hydrothermal synthesis are the important factors affecting the membrane permeability and separation ability. There are two parameters by which to modify the crystal growth during the secondary growth; the pre-aging treatment of the mother liquid and the heating rate to the hydrothermal temperature. To achieve high flux of water and high separation ability, the

effects of pre-aging temperature and the heating rate on the crystal morphology and membrane performance were examined. The pre-aging temperatures of room temperature, 60 °C, and 80 °C with a pre-aging time of 24 h were tested for protection layer formation. After the autoclave temperature reached 180 °C, hydrothermal treatment to form the protection layer (secondary growth) was stopped. Table 4 shows the experimental conditions used for protection layer formation and the separation properties of the membranes using a water/iso-propanol solution. Compared with pre-aging at room temperature (M1), the mordenite membrane prepared using a higher pre-aging temperature had a greater separation factor. On the other hand, compared with 24 h hydrothermal period (M3), the mordenite membrane (M5) showed higher water fluxes meanwhile nearly the same separation factor above 1000.

Figure 5 shows FE-SEM photographs of mordenite nanocrystal-layered membranes in which the protection layer was hydrothermally synthesized after pre-aging of the mother liquid. The crystal size of the mordenite in the protection layer became slightly smaller by increasing the pre-aging temperature from room temperature (M1) to 80 °C (M5). As pre-aging temperature increased, the concentration of the mordenite precursor increased, leading to a small crystal size of mordenite in protection layer. Moreover, increasing the mordenite precursor may improve the crystallinity of mordenite in the protection layer as well as the separation ability of the membrane.

In the next step, the effect of the heating rate from pre-aging temperature to 180°C during hydrothermal synthesis for protection layer formation was examined. Water flux as well as separation factor increased with heating rate from 4.2°C/h (M5) to 6.3°C/h (M6) and M6 showed a separation factor greater than 1900 at each pervaporation

temperature. The Si/Al ratios in the protection layer of the membranes (M1, M5 and M6) are listed in Table 5. In all membranes, the Si/Al ratios of the protection layer are smaller than the Si/Al ratios of the obtained powder after hydrothermal synthesis. This is probably because the seed mordenite crystal preferentially enhanced the crystal growth with higher Al concentration in the frameworks [36]. On the other hand, the Si/Al ratios of the protection layer among these membranes showed almost the same values (Si/Al=5.6~6.5). So these membranes possess almost the same hydrophilicity. By increasing the heating rate to 8.3°C/h (M7), the obtained membrane showed no separation ability. As shown in Fig. 5, micrometer-size mordenite crystals were clearly formed on the nanocrystal layer in membranes M5 and M6. In contrast, the protection layer was not successfully formed in the case of M7 because large pore spaces were observed from the top view of the membrane, leading to no separation ability. It is considered that the hydrothermal synthesis time was too short to form a protection layer dense enough for pervaporation due to insufficient crystal growth. From the top view of the membranes M5 and M6, crystal size in protection layer was decreased by increasing heating rate. By decreasing crystal size in the protection layer, the number of non-zeolitic pores among the mordenite crystals increased, leading to an increase in water flux. In addition, it is considered that the pore space of the interface between nanocrystal layer and protection layer, which is an important area for separation, became small enough to selectively separate water from a water/iso-propanol solution (iso-propanol concentration is 88 wt%). Furthermore, FE-SEM cross-sectional photographs showed that the thickness of the protection layer also decreased with increasing heating rate, which enhanced water flux due to the shorter diffusion length from the feed solution to the interface between the

nanocrystal layer and protection layer. Compared with those of other reports [8, 12, 37], the mordenite nanocrystal-layered membranes prepared in this study exhibits almost the same as or higher in both of the water flux and separation factor. By pre-aging the mother liquid in the high temperature and increasing the heating rate for the protection layer formation, a high performance mordenite membrane with thin layer (protection layer about 1μm) could be successfully synthesized.

[Figure 5, Table 4, Table 5]

4. Conclusions

Mordenite nanocrystal-layered membranes were successfully prepared using the secondary growth method. Mordenite nanocrystals were laminated onto an alumina filter and a mordenite protection layer was clearly formed on the nanocrystal layer. Four types of water/organic solvent solutions were prepared for pervaporation experiments using the mordenite nanocrystal-layered membranes. Permeance of water through the mordenite nanocrystal-layered membrane was similar regardless of the polarity of the organic solvent in the feed solutions however the permeances of the organic molecules depended on their polarities. The mechanisms of water permeation through the mordenite nanocrystal-layered membranes can be considered as the adsorbed water layer formed on both of the zeolitic pores and non-zeolitic pores among crystals for water permeation. The appropriate pore space was formed around the interface between the nanocrystal and protection layer which was expected to be the main separation area of the membranes.

Formation of small size mordenite crystals in the protection layer enhanced the separation ability as well as permeability of the mordenite nanocrystal-layered membranes.

References

1. S. Funai, T. Tago, T. Masuda, Selective production of ketones from biomass waste containing a large amount of water using an iron oxide catalyst, Catalysis Today 164 (2011) 443
2. R.W. Baker, Membrane Technology and Applications, Chapter 9 Pervaporation, McGraw-Hill, 2000
3. F. Mizukami, Catalytic cracking of n-butane over rare earth − loaded HZSM-5 catalysts, Study in Surface Science and Catalysis 125 (1999) 1
4. H. Kita, K. Horii, Y. Ohtoshi, K. Tanaka, K. Okamoto, Synthesis of a zeolite NaA membrane for pervaporation of water/organic liquid mixtures, Journal of Materials Science Letters 14 (1995) 206
5. M. Kondo, M. Komori, H. Kita, K. Okamoto, Tubular-type pervaporation module with zeolite NaA membrane, Journal of Membrane Science 133 (1997) 133
6. K. Okamoto, H. Kita, K. Horii, K. Tanaka, M. Kondo, Tubular-type pervaporation module with zeolite NaA membrane, Industrial & Engineering Chemistry Research 40 (2001) 163
7. T. Sano, M. Hasegawa, Y. Kawakami, H. Yanagishita, Separation of $^{methanol}/_{rmmethyl}$-tert-butyl ether mixture by pervaporation using silicalite membrane, Journal of Membrane Science 107 (1995) 193

8. G. Li, E. Kikuchi, M. Matsukata, The control of phase and orientation in zeolite membranes by the secondary growth method, Microporous and Mesoporous Materials 62 (2003) 211
9. M. Noack, P. Kolsch, J. Caro, M. Schneider, P. Toussaint, I. Sieber, MFI membranes of different Si/Al ratios for pervaporation and steam permeation, Microporous and Mesoporous Materials 35 (2000) 253
10. T. Sano, H. Yanagishita, Y. Kiyozumi, F. Mizukami, K. Haraya, Separation of ethanol/water mixture by silicalite membrane on pervaporation, Journal of Membrane Science 95 (1994) 221
11. T. Masuda, S. Otani, T. Tsuji, M. Kitamura, S.R. Mukai, Preparation of hydrophilic and acid-proof silicalite-1 zeolite membrane and its application to selective separation of water from water solutions of concentrated acetic acid by pervaporation, Separation and Purification Technology 32 (2003) 181
12. X. Lin, E. Kikuchi, M. Matsukata, Preparation of mordenite membranes on α-alumina tubular supports for pervaporation of water–isopropyl alcohol mixtures. Chemical Communication 11 (2000) 957
13. G. Li, E. Kikuchi, M. Matsukata, Separation of water-acetic acid mixtures by pervaporation using a thin mordenite membrane. Separation and Purification Technology 32 (2003) 199
14. A. Navajas, R. Mallada, C. Téllez, J. Coronas, M. Menéndez, J. Santamaría, The use of post-synthetic treatments to improve the pervaporation performance of mordenite membranes, Journal of Membrane Science 270 (2006) 32

15. Y. Cui, H. Kita, K. Okamoto, Zeolite T membrane: preparation, characterization, pervaporation of water/organic liquid mixtures and acid stability, Journal of Membrane Science 236 (2004) 17

16. T. Nagase, Y. Kiyozumi, Y. Hasegawa, T. Inoue, T. Ikeda, F. Mizukami, Dehydration of concentrated acetic acid solutions by pervaporation using novel MER zeolite membranes, Chemistry Letters 36 (2007) 594

17. Y. Kiyozumi, Y. Nemoto, T. Nishide, T. Nagase, Y. Hasegawa, F. Mizukami, Synthesis of acid-resistant Phillipsite (PHI) membrane and its pervaporation performance, Microporus and Mesoporous Materials 116 (2008) 485

18. J. Čejka, J. van Bekkum, A. Corma, F. Schuth, Introduction to zeolite science and Practice, Chapter 6 Zeolite Membranes-Synthesis, Characterization and Application, Elsevier, 2007

19. K. Sato, K. Sugimoto, T. Kyotani, N. Shimotsuma, T. Kurata, Synthesis, reproducibility, characterization, pervaporation and technical feasibility of preferentially b-oriented mordenite membranes for dehydration of acetic acid solution, Journal of Membrane Science 385-386 (2011) 20

20. M. Matsukata, K. Sawamura, T. Shirai, M. Takada, Y. Sekine, E. Kikuchi, Controlled growth for synthesizing a compact mordenite membrane, Journal of Membrane Science 316 (2008) 27

21. G. Li, E. Kikuchi, M. Matsukata, The control of phase and orientation in zeolite membranes by the secondary growth method, Microporous and Mesoporous Materials 62 (2003) 218

22. Q. Li, B. Mihailova, D. Creaser, J. Sterte, Aging effects on the nucleation and crystallization kinetics of colloidal TPA-silicalite-1, Microporous and Mesoporous Materials 43 (2001) 51

23. H. Chen, C. Song, W, Yang, Effects of aging on the synthesis and performance of silicalite membranes on silica tubes without seeding, Microporous and Mesoporous Materials 102 (2007) 250

24. M.M. Nia, H. Amiri, Measurement and modeling of static dielectric constants of aqueous solutions of methanol, ethanol and acetic acid at T=293.15 K and 91.3 kpa, The Journal of Chemical Thermodynamics 57 (2013) 68

25. G. Åkerlöf, Dielectric constants of some organic solvent-water mixtures at various temperatures, Journal of the American Chemical Society 54 (11) (1932) 4125

26. C.G. Malmberg, A.A. Maryott, Dielectric constant of water from 0 º to 100 ºC, Journal of research of the National Bureau of Standards 56 (1) (1956) 2641

27. T. Tago, Y. Nakasaka, A. Kayoda, T. Masuda, Preparation of hydrophilic silicalite-1 nanocrystal-layered membrane for separation of water from water-acetone solution by pervaporation, Separation and Purification Technology 58 (2007) 7

28. T. Tago, Y. Nakasaka, A. Kayoda, T. Masuda, Preparation of hydrophilic silicalite-1 nanocrystal-layered membrane and their application to separating water from water-acetone solution. Microporous and Mesoporous Materials 115 (2008) 176

29. T. Tago, D. Aoki, K. Iwakai, T. Masuda, Preparation for Size-Controlled MOR Zeolite Nanocrystal using Water/Surfactant/Organic Solvent, Topics in Catalysis 52 (2009) 865

30. X. Li, H. Kita, H. Zhu, Z. Zhang, K. Tanaka, Synthesis of long-term acid-stable zeolite membranes and their potential application to esterification reaction, Journal of Membrane Science 339 (2009) 224

31. A.K. Pabby, S.S.H. Rizvi, A.M. Sastre, Handbook of Membrane Separations, 2008, P289

32. M. Nomura, T. Yamaguchi, S. Nakao, Transport phenomena through intercrystalline and intracrystalline pathways of silicalite zeolite membranes, Journal of Membrane Science 187 (2001) 203

33. T.C. Bowen, R.D. Noble, J.L. Falconer, Fundamentals and applications of pervaporation through zeolite membranes, Journal of Membrane Science 245 (2004) 15

34. T.C. Bowen, H. Kalipcilar, J.L. Falconer, R.D. Noble, Pervaporation of Organic/water mixtures through B-ZSM-5 zeolite membranes on monolith supports, Journal of Membrane Science 215 (2003) 235

35. K. Okamoto, H. Kita, K. Horii, K. Tanaka, M. Konodo, zeolite NaA membrane: preparation, single-gas permeation, and pervaporation and vapor permeation of water/organic liquid mixtures, Industry and Engineering Chemistry Research 40 (2001) 163

36. M. Noack, P. Kölsch, V. Seefeld, P. Toussaint, G. Georgi, J. Caro, Influence of the Si/Al-ratio on the permeation properties of MFI-membranes, Miroporous and Mesoporous Materials 79 (2005) 329

37. Y.F. Zhang, Z.Q. Xu, Q.L. Chen, Synthesis of small crystal polycrystalline mordenite membrane, Journal of Membrane Science 210 (2002) 361

Figure and Table Legends

Figure 1: Schematic of the stainless steel autoclave vessel used for pervaporation experiments.

Figure 2: FE-SEM photographs of mordenite nanocrystal-layered membranes: cross-sectional area.

Figure 3: XRD patterns of (a) commercial mordenite, and powders obtained in solution after protection layer formation at (b) 150 ˚C (c) 180 ˚C, and (d) 200 ˚C.

Figure 4: Permeance of water (circles) and organic molecules (triangles) through a mordenite nanocrystal-layered membrane. The solid line is water permeance from water (without organics) through the mordenite nanocrystal-layered membrane.

Figure 5: FE-SEM photographs of mordenite nanocrystal-layered membranes, containing a protection layer synthesized after pre-aging of the mother liquid: (a) top view, (b) cross-sectional area, (c) interface area by large magnification.

Table 1: Apparent activation energy of the water flux through a mordenite nanocrystal-layered membrane from a water/organic solvent solution and the dielectric constant of the organic solvents.

Table 2: Effect of hydrothermal temperature on membrane separation property from water/iso-propanol solution.

Table 3: Pervaporation experiment for separation water from acetic acid/water mixtures

Table 4: Experimental conditions for formation of the protection layer and separation properties of the membranes prepared.

Table 5: Si/Al ratio of protection layer in mordenite membrane

5

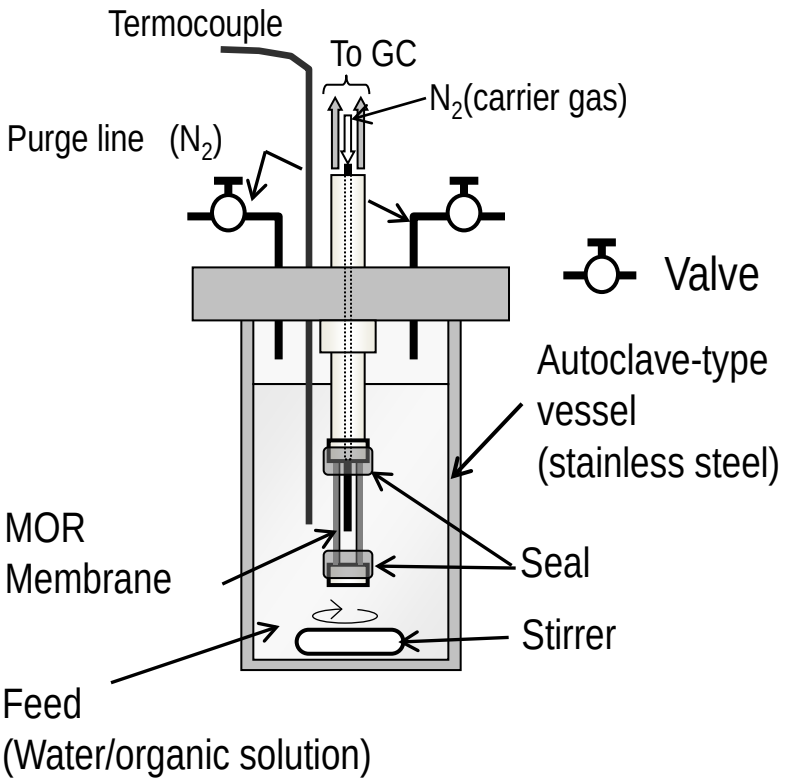

Figure 1 Schematic of the stainless steel autoclave vessel used for pervaporation experiments.

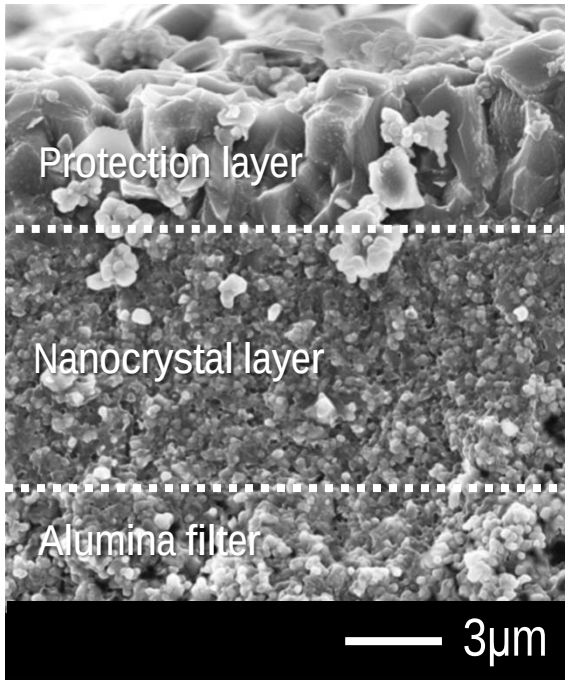

Figure 2 FE-SEM photographs of mordenite nanocrystal-layered membrane (cross-sectional area), (prepared at a hydrothermal temperature of 180 ˚C in Table 2).

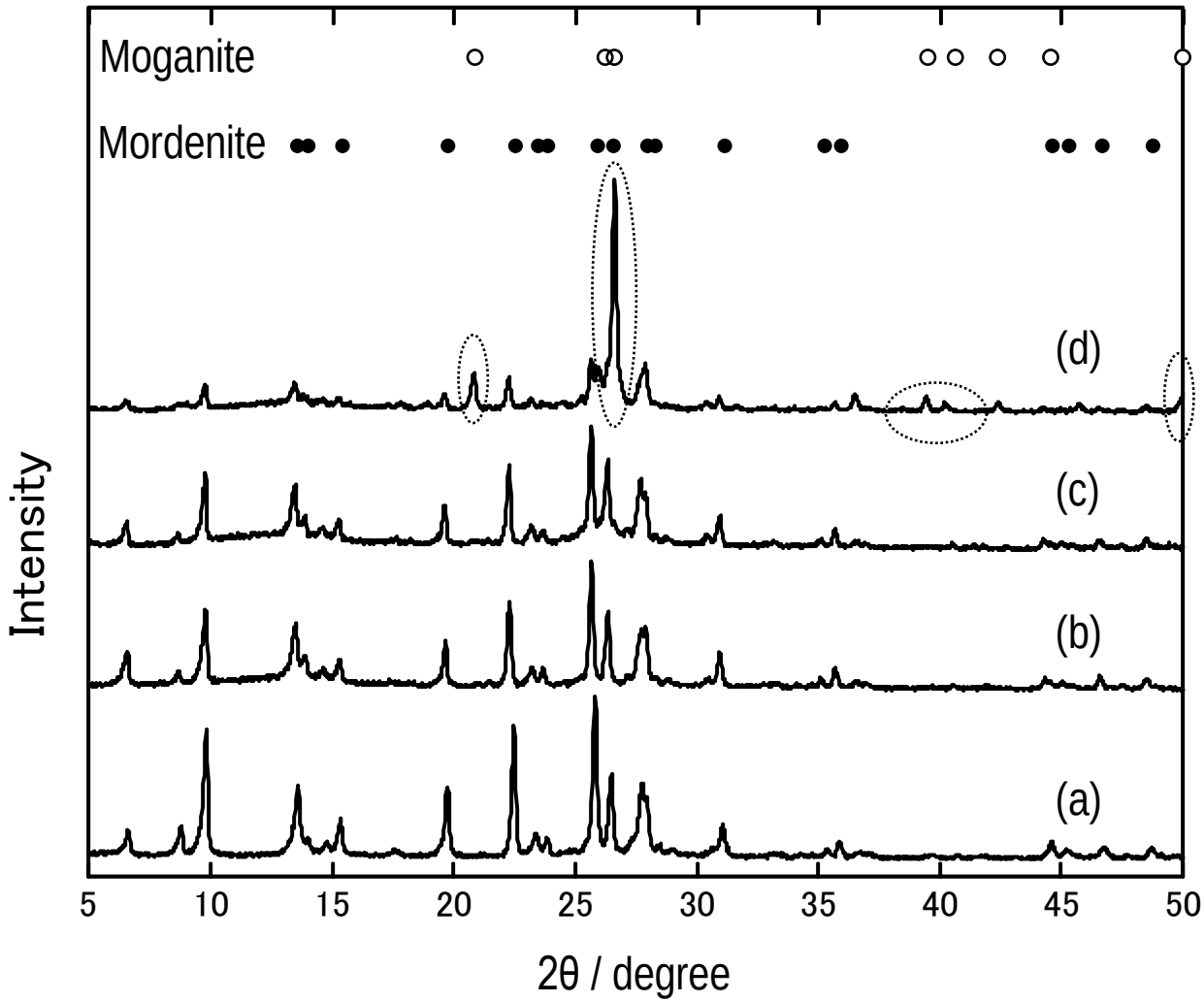

Figure 3 XRD patterns of (a) commercial mordenite, and powders obtained in solution after protection layer formation at (b) 150˚C (c) 180˚C and (d) 200˚C

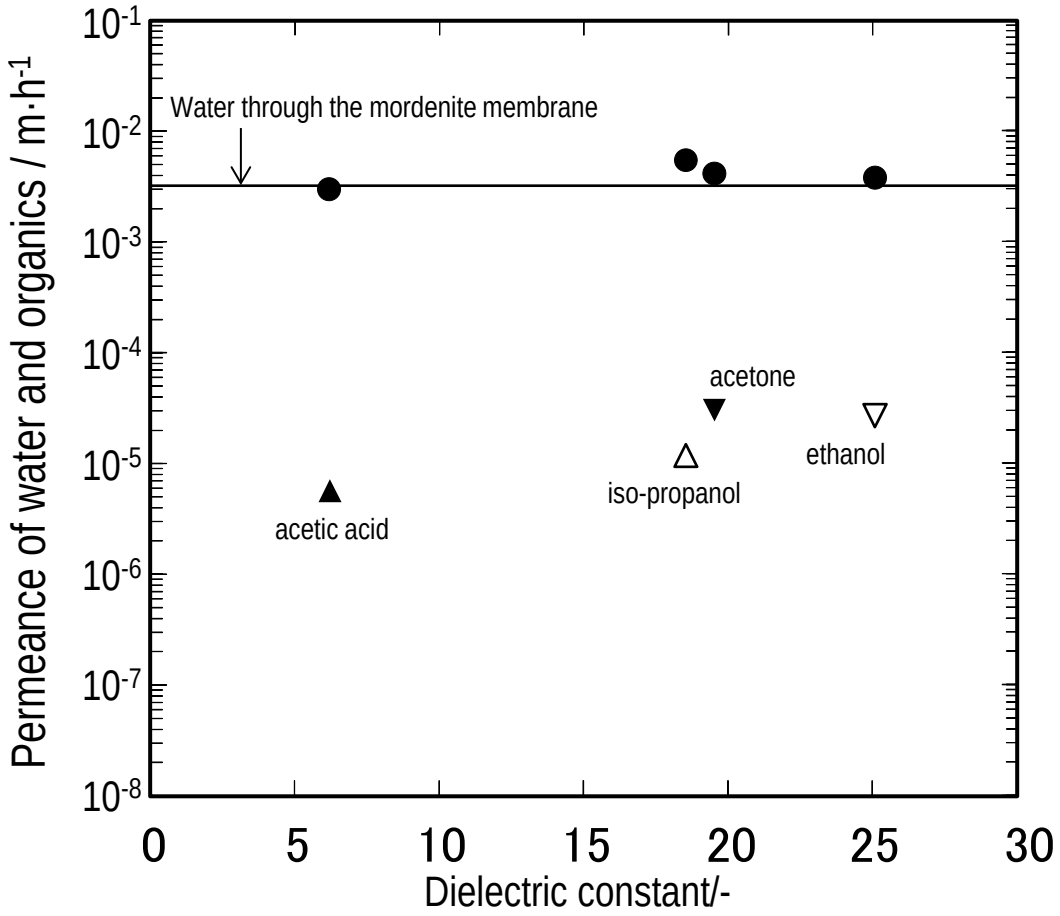

Figure 4 Permeance of water (circles) and organic molecules (triangles) through a mordenite nanocrystal-layered membrane. The solid line is water permeance from water (without organics) through the mordenite nanocrystal-layered membrane.

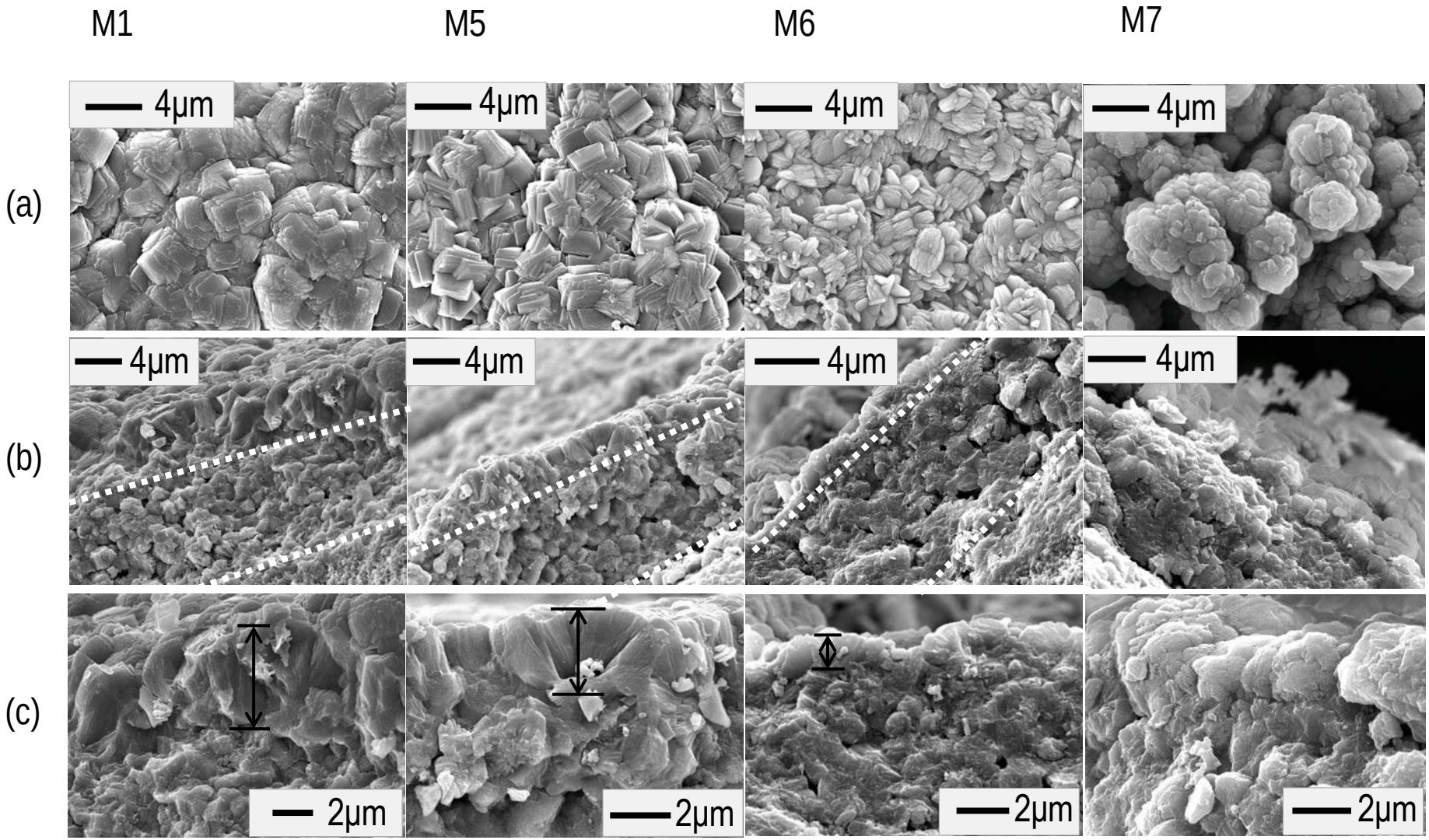

Figure 5 FE-SEM photographs of mordenite nanocrystal-layered membranes, containing a protection layer synthesized after pre-aging of the mother liquid: (a) top view, (b) cross-sectional area, and (c) interface area by large magnification.

Table 1 Apparent activation energy of the water flux through a mordenite nanocrystal-layered membrane from a water/organic solvent solution and the dielectric constant of the organic solvents.

Organic solvent	Organic concentration in solution (wt%)	Dielectric constant (-)**	Apparent activation energy ($kJ \cdot mol^{-1}$)
ethanol	90	25.02 [24]	38
acetone	90	19.56 [25]	30
iso-propanol	88	18.62 [25]	32
acetic acid	90	6.15 [24]	41
water*	—	80.1 [26]	38

*apparent activation energies of water flux through the membranes from water (without organic solvent)

** the dielectric constant at 20 ºC

Table2 Effect of hydrothermal temperature on membrane separation property from water/iso-propanol solution.

Pre-aging		Hydrothermal synthesis conditions				Water flux through the membrane (kg $m^{-2}h^{-1}$)	Separation factor (-)
Temperature (^oC)	Period (h)	Heating Rate (^oC/h)	Heating Period (h)	Hydrothermal temperature (^oC)	Hydrothermal Period (h)		
R.T.	24	5.0	24	150	12	0.199	648
R.T.	24	6.3	24	180	12	0.254	734
R.T.	24	7.1	24	200	12	0.186	538

* Feed: iso-propanol/water solution (88 wt%), pervaporation temperature:80 ˚C

Table3 Pervaporation experiments for separation water from acetic acid/water mixtures.

Pervaporation time period (h)	5.8	12.3	25.8	32.6
Water flux through the membrane (kg $m^{-2}h^{-1}$)	0.179	0.195	0.159	0.133
Separation factor (-)	83	90	138	158

* Feed: acetic acid/water solution (90 wt%), pervaporation temperature:100 ˚C.

Table 4 Experimental conditions for formation of the protection layer and separation properties of the membranes prepared.

Sample	Pre-aging		Hydrothermal synthesis conditions			Pervaporation temperature					
						60 °C		80 °C		100 °C	
	Temperature (°C)	Period (h)	Heating rate (°C/h)	Heating Period (h)	Hydrothermal Period (h)	F_w [a]	α [b]	F_w [a]	α [b]	F_w [a]	α [b]
M1	R.T.	24	6.3	24	0	0.147	420	0.383	400	0.459	130
M2	R.T.	24	6.3	24	12	0.137	1200	0.254	730	0.454	470
M3	R.T.	24	6.3	24	24	0.126	1800	0.237	1200	0.423	1000
M4	60	24	5.0	24	0	0.293	570	0.482	330	0.664	170
M5	80	24	4.2	24	0	0.322	1420	0.455	1370	0.597	1170
M6	80	24	6.3	16	0	0.435	1920	0.806	2020	1.013	2600
M7	80	24	8.3	12	0	>1	—	>1	—	>1	—

* Feed: iso-propanol/water solution (88 wt%)

a: water flux through the membrane (kg $m^{-2}h^{-1}$).

b: separation factor (-).

Table5 Si/Al ratio of protection layer in mordenite membrane

Samples	Si/Al ratio of powder obtained in the solution during hydrothermal synthesis (mol%) *	Si/Al ratio of as-synthesized mordenite membrane (mol%) **
M1	10.3	6.48
M5	9.75	5.63
M6	8.87	5.87

* Analyzed by XRF

** Analyzed by EDS